Journal of Cellular Physiology

H-Ras and PI3K Are Required for the Formation of Circular Dorsal Ruffles Induced by Low-Power Laser Irradiation

XUEJUAN GAO, DA XING,* LEI LIU, AND YONGHONG TANG

MOE Key Laboratory of Laser Life Science, Institute of Laser Life Science, South China Normal University, Guangzhou, China

The formation of circular dorsal ruffles upon growth factor stimulation facilitates the static cells for subsequent motility. Low-power laser irradiation (LPLI) has been shown to exert some promotive effects on migration and proliferation in various cell types. It is unclear whether LPLI could induce the formation of circular ruffles. In this study, using confocal fluorescence microscope, we for the first time demonstrated that LPLI could induce the production of circular ruffle structures in COS-7 cells. These structures were proved to be actin-based and originated from membrane microdomains enriched in cholesterol. Ras was shown to be activated by LPLI and expression of YFP-H-Ras (N17), a dominant negative H-Ras, blocked the generation of circular ruffles induced by LPLI. Wortmannin, PI3K inhibitor, potently suppressed the formation of LPLI-induced circular ruffles in a dose-dependent manner. However, blocking the activation of PKC, which was activated during LPLI-induced cell proliferation in our previous study, had no effect on the formation of circular ruffles. Thus, both H-Ras and PI3K were required for the formation of circular ruffles induced by LPLI and the generation of circular ruffles provides new information for the mechanisms of biological effects of LPLI.

J. Cell. Physiol. 219: 535–543, 2009.

The plasma membrane can be modified into distinct, ordered structures under specific physiological conditions (Buccione et al., 2004). Circular dorsal ruffles or "waves" are dynamic and transient actin-based structures that often form in response to stimulation of receptor tyrosine kinases, including epidermal growth factor receptor (EGFR), platelet-derived growth factor, and hepatocyte growth factor receptors (HGFRs) (Mellstrom et al., 1988; Dowrick et al., 1993; Shinohara et al., 2002; Buccione et al., 2004). The occurring of circular dorsal ruffles/waves typically does not form until minutes after stimulation and they form only once, lasting 5–20 min (Buccione et al., 2004). Currently, the numerous cellular roles of circular dorsal ruffles have been reported, such as preparing a static cell for subsequent movement (Krueger et al., 2003), macropinocytosis (Dowrick et al., 1993; Araki et al., 2000), and internalizing ligand-bound EGFR from the dorsal plasma membrane (Orth et al., 2003, 2006). It has also been indicated that circular ruffles facilitate the reorganization of the actin cytoskeleton associated with lamellipodia of cells, which could direct cell motility and support extension of the lamellipodial edge (Safiejko-Mroczka and Bell, 2001; Krueger et al., 2003).

Several protein kinases are localized to circular ruffles and participate in their formation and function. The activations of EGFR and its immediate effector kinase, PI3K, are required for circular ruffle formation (Orth et al., 2006). Several small GTPases, such as Ras, Rac, and Rab5, have been implicated in the formation of circular ruffles. Expressions of inactive, GDP-bound forms of them inhibit circular ruffling (Lanzetti et al., 2004).

Low-power laser irradiation (LPLI) shows some promotive effects on migration and proliferation in various cell types, and induces the phosphorylation of tyrosine protein kinase receptor (TPKR), such as c-Met, HGFR (Shefer et al., 2001, 2002; Gao et al., 2006; Tuby et al., 2007; Chen et al., 2008). Ras, the immediate effector of TPKR, coordinates a variety of cellular responses to extracellular stimuli and regulates cell proliferation and differentiation (Bivona and Philips, 2003; Kupzig et al., 2005). Moreover, Ras induces the rearrangements of actin cytoskeleton and the alterations of cell morphology (Crespi et al., 2002). However, it has not been examined whether LPLI could induce the formation of circular dorsal ruffles and whether Ras could be activated by LPLI.

In this study, we for the first time confirmed the formation of circular ruffles induced by LPLI. Ras was shown to be activated by LPLI and involved in the formation of LPLI-induced circular ruffles. Both H-Ras and PI3K were required for the circular ruffle formation. The detailed regulation of these structures will be discussed in the context.

Materials and Methods

Reagents

Cytochalasin D (CD) was purchased from Sigma (St. Louis, MO). Cholera toxin subunit B (CT-B) Conjugates was purchased from Molecular Probes (Invitrogen, Carlsbad, CA). Epidermal growth factor (EGF) was purchased from PeproTech (Rocky Hill, NJ). Gö 6983 was purchased from Merck (Darmstadt, Germany). Wortmannin was purchased from BIOMOL Research Laboratories, Inc. (Plymouth, PA). Lipofectamin 2000 was from Invitrogen.

Cell culture and transfection

COS-7 cells were cultured in Dulbecco's modified Eagle medium (DMEM, Gibco BRL, Grand island, NY) with 10% fetal calf serum at

Contract grant sponsor: National Natural Science Foundation of China;
Contract grant number: 30627003 30870676.
Contract grant sponsor: Natural Science Foundation of Guangdong Province;
Contract grant number: 7117865.

*Correspondence to: Da Xing, MOE Key Laboratory of Laser Life Science, Institute of Laser Life Science, South China Normal University, Guangzhou 510631, China. E-mail: xingda@scnu.edu.cn

Received 27 October 2008; Accepted 9 December 2008

Published online in Wiley InterScience (www.interscience.wiley.com.), 13 January 2009.
DOI: 10.1002/jcp.21693

37°C in a humidified atmosphere containing 5% CO_2. Cells at a 40–60% confluence were transfected with Lipofectamin 2000. Green fluorescent protein (GFP)-H-Ras and yellow fluorescent protein (YFP)-H-Ras (N17) plasmids were kindly provided by Prof. Piero Crespo and Prof. Thomas Schmidt, respectively. Plasmid DNA of Raichu-Ras was presented by Prof. Michiyuki Matsuda.

Laser scanning microscope (LSM)

Live cell imaging experiments were performed on laser scanning microscopes (LSM510/ConfoCor2) combination system (Zeiss, Jena, Germany) equipped with a Zeiss Plan-Neofluar 40×/1.3 NA Oil Dic objective (Gao et al., 2006; Zhang et al., 2008). The stage of LSM was equipped with a temperature-controlled and CO_2-controlled small incubator (CTI-controller 3700 digital and Tempcontrol 37–2 digital, Zeiss), which maintains the cells at 37°C, 5% CO_2 during the whole experiment. GFP or YFP was excited with 488 or 514 nm Ar-Ion laser, and fluorescence emission was detected through a 500–550 nm band-pass filter or a 530 nm long-pass filter, respectively. During the experiments, the exciting power of 488 nm or 514 nm laser was reduced to the minimal level (0.5–1%) to reduce the possible effects of exciting light.

EGF, 5% serum, and LPLI treatments

COS-7 cells cultured on coverslip-bottomed small chamber were transfected with GFP-H-Ras or YFP-H-Ras (N17) and starved for at least 24 h in Earle's balanced salt solutions (EBSS). For single-cell analysis, the small chamber was mounted onto the stage of LSM microscope and then treated with EGF (50 ng/ml), serum (5%), or irradiated with He–Ne laser (Guangzhou, China; 632.8 nm, 16 mW/cm^2, 50 sec, 0.8 J/cm^2). The images before and after the individual treatment were acquired by LSM microscope. For statistical analysis, about 40 min after EGF, 5% serum or LPLI treatment, the cells were fixed in 4% formaldehyde for 15 min, washed three times 5 min each with phosphate-buffered saline (PBS) containing 100 mM glycine, and then observed by LSM microscope.

To depolymerize actin filaments, the cells were pretreated with CD (10 μM, diluted in dimethyl sulfoxide) for 1 h. To inhibit the activation of PI3K or PKC, the cells were pretreated with wortmannin (1 μM or 100 nM, diluted in dimethyl sulfoxide) or Gö 6983 (1 μM, diluted in dimethyl sulfoxide) for 30 min, respectively. Then the cells were used to do the designed experiments.

CT-B uptake study

COS-7 cells expressing GFP-H-Ras were starved for 24 h and treated with EGF (50 ng/ml) or LPLI (0.8 J/cm^2) for 10 min, respectively. Then, the cells were incubated for 30 min at 4°C in EBSS containing 0.5 μg/ml CT-B-Alexa 594 and observed by LSM microscope. Dye Alexa 594 was excited with 633 nm He–Ne laser (Zeiss), and fluorescence emission was detected through a 650 nm long pass filter.

Immunofluorescence

Cells were cultured on coverslips, fixed in 4% formaldehyde for 15 min, washed three times 5 min each with PBS containing 100 mM glycine, and permeabilized for 4 min in 0.1% Triton X-100/PBS. Cells were stained with 1:50 anti-β-actin antibody (SC-47778; Santa Cruz Biotechnology, Santa Cruz, CA) overnight at 4°C and with secondary antibody of Alexa Fluor 680® goat anti-mouse IgG (Molecular Probes) for 60 min, following with three washes in PBS between every step. Coverslips were viewed by LSM microscope. Alexa Fluor 680® was excited with 633 nm He–Ne laser, and fluorescence emission was detected through a 650 nm long pass filter.

The expression of Raichu-Ras reporter in COS-7 cells

COS-7 cells transfected with Raichu-Ras plasmid and control untransfected cells were lysed, and cell lysates were subjected to SDS–PAGE, transferred to BioTrace™ NT Nitrocellulose Membranes (Pall). The resulting membranes were incubated with the monoclonal anti-Ras anti-Ras antibody (Cell Biolabs, San Diego, CA) and anti-β-actin antibody (Santa Cruz Biotechnology, SC-47778), and with the secondary antibody Alexa Fluor 680® goat anti-mouse IgG (Molecular Probes). The signals were detected with an ODYSSEY® Infrared Imaging System (Li-Cor, NE).

Spectrofluorometric analysis of Ras activity after LPLI or EGF treatment in living cells

COS-7 cells transfected with Raichu-Ras reporter were starved for 24 h and treated with nothing (control), LPLI (He–Ne laser, 16 mW/cm^2, 0.8 J/cm^2), or EGF (50 ng/ml), respectively. Then these cells were immediately transferred into a 96-well microplate. The fluorescence emission spectra of Raichu-Ras were obtained by performing the Tecan Infinite M200 Microplate Reader. Excitation of the cells was at 433 nm (5 nm bandwidth), and the emission spectra of the cells were collected with a bandwidth of 20 nm. The corresponding background spectra of cell-free culture medium were subtracted.

Ras activation assay

Ras activation assay kit was purchased from Cell Biolabs, containing Raf11 RBD Agarose, mouse monoclonal anti-Ras, GTPase immunoblot positive control. COS-7 cells cultured in petri dish with a diameter of 6 cm were starved for 24 h and then treated with LPLI (semiconductor laser, nLight Corporation, Shanghai, China; 635 nm, 16 mW/cm^2, 0.8 J/cm^2) and EGF (50 ng/ml), respectively. After 20 min of treatment with LPLI or 15 min of incubation with EGF, the cells were lysed and pull-down assay was performed using whole cell lysates as per the manufacturer's instructions. Supernatant after pull-down were resolved by 15% SDS–PAGE, transferred to nitrocellulose membranes, incubated with mouse monoclonal anti-Ras and the secondary antibody Alexa Fluor 680® goat anti-mouse IgG (Molecular Probes), and visualized using an ODYSSEY Infrared Imaging System.

Results

The formation of circular ruffles stimulated by EGF and 5% serum

To investigate the effects of LPLI on circular ruffle formation, we first confirm the formation of circular ruffles stimulated by EGF. COS-7 cells transfected with GFP-H-Ras were starved for at least 24 h and then treated with EGF. It has been long known that the biostimulatory effects of LPLI could be more pronounced in cells with a low metabolic rate (Karu, 1999), thus, in our experiments the cells were rendered quiescent by serum starvation for 24 h. Confocal microscopy revealed that before EGF (0 min), GFP-H-Ras was uniformly localized to the whole cell except that a fraction of H-Ras localized adjacent to the nucleus (Fig. 1A). Ten minutes after EGF, the peripheral linear ruffles were observed (arrow). After 30 min of EGF stimulation, circular ruffles were generated along peripheral cell edges (arrows) as well as in the center of cell. The magnified images showed that the circular ruffles expanded outside, swept across the cell, and changed into half ring-shaped or arc-shaped structures (Fig. 1B). These structures were transient and disappeared within 5–20 min, consistent with the reported lasting time (Buccione et al., 2004). Next, we tested the colocalization of circular ruffles with F-actin by immunofluorescence assay. After 40 min of EGF stimulation, the circles containing GFP-H-Ras along peripheral cell edges colocalized with the F-actin (Fig. 1C, arrows). Since the principal

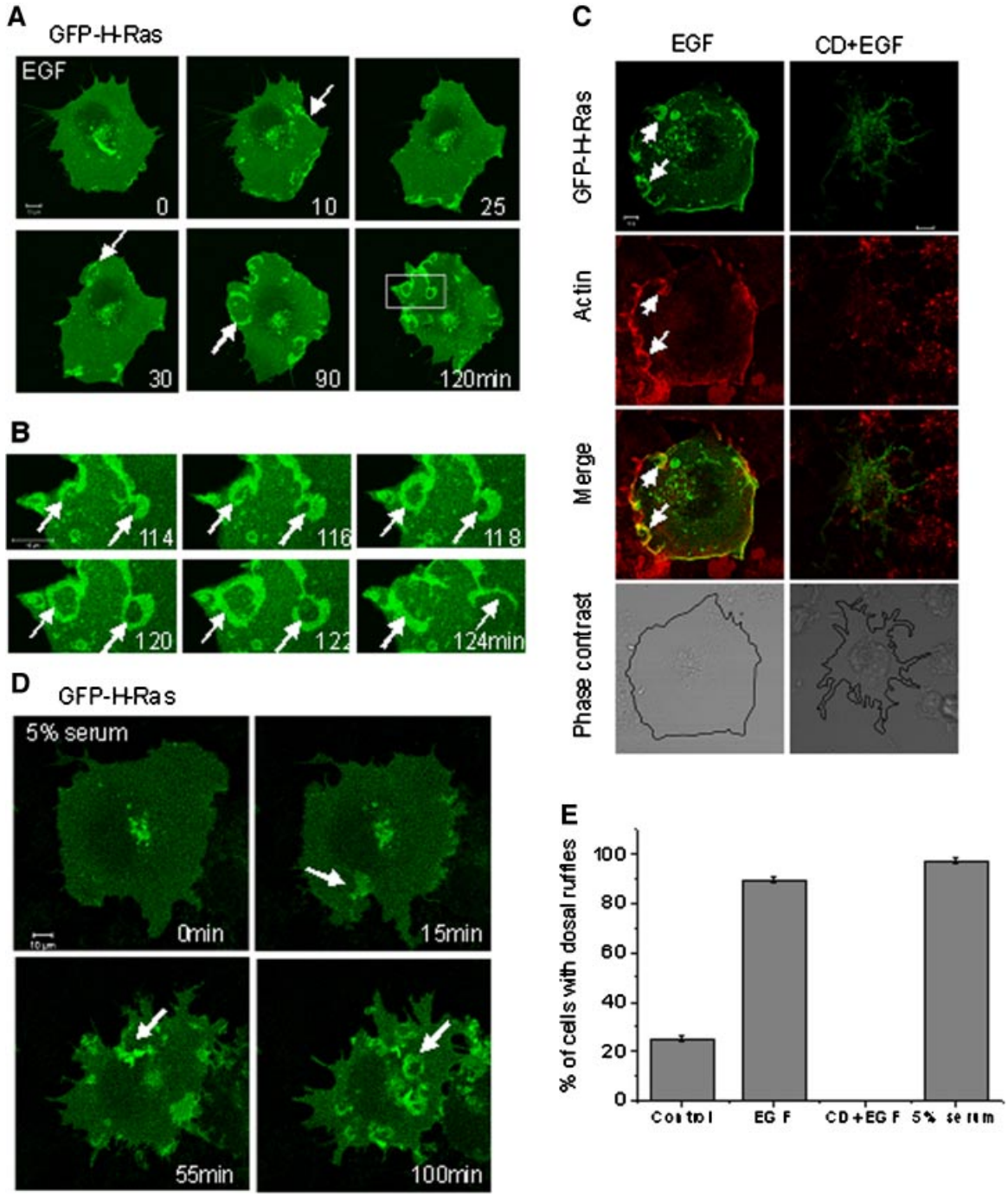

Fig. 1. The formation of circular ruffles induced by EGF and 5% serum. A: Time-series images after EGF stimulation. COS-7 cells were transfected with GFP-H-Ras and starved for at least 24 h. Then, the cells were treated with EGF (50 ng/ml) and recorded by LSM510 microscope. B: Selected image series of region of interest (ROI) indicated by the white rectangle in (A). C: About 40 min after EGF (50 ng/ml) with or without CD pretreatment, the cells expressing GFP-H-Ras were fixed, permeabilized, and stained for F-actin. Colocalization on the merged images looks yellow. D: Time-series images after serum (5%) stimulation. COS-7 cells transfected with GFP-H-Ras after starvation were treated with 5% serum and recorded by LSM microscope. E: COS-7 cells expressing GFP-H-Ras were starved for 24 h and then treated with nothing (control), EGF, CD before adding EGF, and 5% serum, respectively. About 40 min after EGF or 5% serum stimulation, the cells were fixed and the percentage of cells generating at least one circular ruffle was determined. For each condition, >100 cells were counted, and each represented the average value from three independent experiments (mean ± SD). Bars: 10 μm. [Color figure can be viewed in the online issue, which is available at www.interscience.wiley.com.]

structural component of circular ruffles was actin, the circles were indeed circular ruffle structures. Therefore, this result confirmed previous reports that EGF could induce the circular ruffle formation in COS-7 cells and other cells (Shinohara et al., 2002; Buccione et al., 2004; Orth et al., 2006). After depolymerizing the F-actin with CD, a known F-actin depolymerizing agent, the cells rounded up gradually, and the generation of circular ruffles was abolished (Fig. 1C), indicating

that the formation of the circular ruffles containing H-Ras was actin-based.

Subsequently, we tested whether 5% serum stimulation could also induce the generation of circular ruffles. Confocal microscopy revealed that at about 15 min of 5% serum stimulation, the cell began to generate circular ruffles, especially obvious after 55 min (Fig. 1D, arrows). The percentage of cells with circular ruffles showed that in control condition, ~25% of cells expressing GFP-H-Ras produced circular ruffles (Fig. 1E). Nearly 90% of cells generated circular ruffles after EGF stimulation. But when the cells were pretreated with CD, the generation of circular ruffles was abolished. When stimulated by 5% serum, nearly 97% of cells generated circular ruffles. Thus, these results demonstrated that exogenous expression of GFP-H-Ras only could cause the production of a small number of circular ruffles and the production was strongly enhanced by EGF and 5% serum stimulations. Numerous roles have been attributed to circular ruffles, including preparing a static cell for subsequent movement (Krueger et al., 2003). It was notable that the formation of these structures promoted the changes in cell shape, which would facilitate the static cell activation.

The formation of circular ruffles induced by LPLI

We next examine whether LPLI could induce the formation of circular dorsal ruffles. For this purpose, COS-7 cells transfected with GFP-H-Ras were serum starved and treated with LPLI (0.8 J/cm^2). 0.8 J/cm^2 is a typical fluence of LPLI to induce ASTC-a-1 cell proliferation in our previous study (Gao et al., 2006). Confocal microscopy revealed that 40 min after irradiation, the circular ruffles containing H-Ras were generated along peripheral cell edges and also emerged in the center of the cell over time (Fig. 2A, arrows). The circular ruffles typically expanded outside, swept across the cell, and changed into half ring-shaped or arc-shaped structures (Fig. 2B, arrows), consistent with the changes happened in EGF-treated cells. Therefore, LPLI could induce the formation of circular ruffle containing H-Ras in COS-7 cells.

The result of colocalization of LPLI-induced circular ruffles with F-actin showed that about 40 min after irradiation, the arc-shaped circular ruffle containing GFP-H-Ras colocalized well with the F-actin (Fig. 2C, arrows). When we depolymerized F-actin with CD, the generation of circular ruffles was blocked (Fig. 2C). Thus, the formation of LPLI-induced circular ruffles was actin-based.

Then, we investigated whether circular ruffle structures came from plasma membrane. The B subunit of cholera toxin (CT-B) is used as a marker for lipid rafts, which are membrane microdomains enriched in cholesterol and segregate specific groups of proteins, thereby providing a hub for cellular signaling and protein trafficking (Janes et al., 1999). As shown in Figure 2D, the produced arc-shaped circular ruffles after LPLI or EGF stimulation colocalized well with the CT-B conjugate (arrows), suggesting that these structures originated from microdomains enriched in cholesterol of the plasma membrane.

The percentage of cells with circular ruffles showed that in control condition, ~25% of cells expressing GFP-H-Ras produced circular ruffles (Fig. 2E). When stimulated by LPLI, the percentage increased and ~75% of cells generated these structures. However, pretreatment with CD completely blocked dorsal ruffle production. Thus, the production of circular ruffles was strongly enhanced by light stimulation. It was possible that through inducing the generation of circular ruffles, LPLI changed the cell morphology, and activated the static cells.

To directly observe the effect of LPLI on circular ruffle formation, we stained F-actin in the cells without GFP-H-Ras transfection by immunofluorescence assay, showing in suit occurring of circular dorsal ruffles. After starvation, COS-7 cells were treated with nothing (control), LPLI, or EGF, respectively. About 40 min after LPLI or EGF, the control untreated cells had no circular ruffles, consistent with cells requiring agonist stimulation to generate dorsal ruffles (Fig. 2F). In LPLI- and EGF-treated groups, the percentages of cells with circular ruffles were 26% and 35%, respectively. Thus, these results directly indicated the generation of LPLI-induced circular ruffles in COS-7 cells.

The activation of Ras induced by LPLI

Since H-Ras was involved in the formation of circular ruffles induced by LPLI, we next examined whether Ras could be activated by LPLI. For this purpose, fluorescence resonance energy transfer (FRET)-based Raichu-Ras reporter was used (Fig. 3A) (Mochizuki et al., 2001). To test whether Raichu-Ras reporter could express correctly in COS-7 cells, a monoclonal anti-Ras antibody was used. Our result showed that in cells transfected with Raichu-Ras reporter, a band about 84 kDa, corresponding to the expression of Raichu-Ras, was detected (Fig. 3B). In untransfected control cells, this band was not observed. Both actin and endogenous Ras were detected in transfected cells and control cells. This result showed that Raichu-Ras reporter could be expressed correctly in COS-7 cells.

To confirm the activation of Ras in living cells induced by LPLI, we measured the changes in fluorescence emission spectra of Raichu-Ras in response to LPLI and EGF treatments. EGF can effectively activate Ras (Jiang and Sorkin, 2002; Mochizuki et al., 2001). The spectrometer showed that the emission peak of CFP decreased, and the emission peak of YFP increased after 15 min of treatment with EGF, which indicated the increased FRET efficiency and the increased activation of Ras (Fig. 3C, right column). As shown in Figure 3C middle column, Ras activation was increased after 20 min of treatment with LPLI. In contrast, Ras activation was not observed in control untreated cells (Fig. 3C, left column). Taken together, these results indicated that Ras was activated by LPLI in living cells.

To further demonstrate the activation of Ras induced by LPLI, pull-down assay was used. COS-7 cells were starved for 24 h and treated with LPLI and EGF, respectively. Then the cells were lysed and pull-down assay was performed using whole cell lysates. The amount of GTP-bound Ras in cell lysates was determined by affinity precipitation with the Raf11 RBD Agarose beads that has several times higher binding affinity to GTP-Ras than to GDP-Ras. As shown in Figure 3D (quantified in bottom part), Ras in LPLI- and EGF-treated cells but not in control non-treated cells were pulled down by RBD Agarose beads, thus indicating that endogenous Ras was activated by LPLI.

Then, we used YFP-H-Ras (N17), a dominant negative H-Ras, to investigate the effects of H-Ras activation on the formation of circular ruffles. As shown in Figure 3E, expression of YFP-H-Ras (N17) blocked the generation of circular ruffles induced by LPLI or EGF, but did not inhibit peripheral linear ruffle formation (arrows). When >100 cells containing YFP-H-Ras (N17) were counted after LPLI or EGF treatment, no circular ruffles were observed (data not shown), consistent with the reported results that expression of inactive, GDP-bound forms of Ras inhibits circular ruffling (Lanzetti et al., 2004). Thus, H-Ras activation was required for the formation of circular ruffles induced by LPLI or EGF.

PI3K, not PKC involved in the regulation of circular ruffle formation

It has been reported that PI3K was involved in cell proliferation induced by LPLI (Shefer et al., 2003), we next investigate the

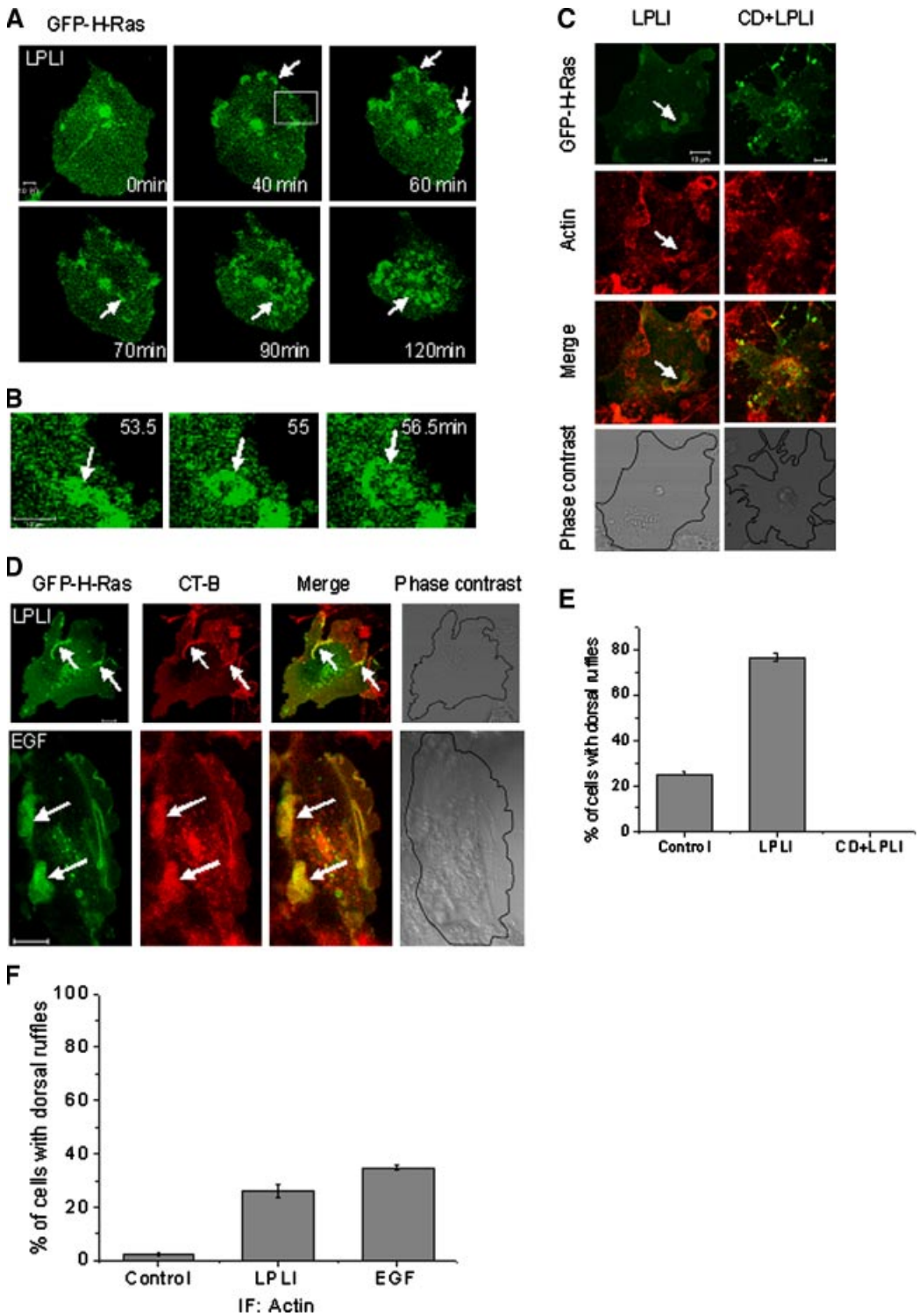

Fig. 2. The formation of circular ruffles induced by LPLI. A: Time-series images after LPLI. COS-7 cells were transfected with GFP-H-Ras and starved for 24 h. Then, the cells were treated with He–Ne laser (0.8 J/cm^2) and recorded by LSM microscope. B: Selected image series of ROI indicated by the white rectangle in (A). C: 40 min after LPLI (0.8 J/cm^2) with or without CD pretreatment, the cells expressing GFP-H-Ras were fixed, permeabilized, and stained for F-actin. D: Colocalization of the circular ruffle structures with the lipid marker CT-B-Alexa 594. COS-7 cells expressing GFP-H-Ras after starvation were treated with LPLI or EGF, respectively, and then incubated with 0.5 μg/ml CT-B-Alexa 594. Colocalization on the merged images looks yellow. E: COS-7 cells expressing GFP-H-Ras were starved and then treated with nothing (control), LPLI (0.8 J/cm^2), CD before adding LPLI (0.8 J/cm^2), respectively. About 40 min after irradiation, the cells were fixed and the percentage of cells generating at least one circular ruffle was determined. F: COS-7 cells without GFP-H-Ras transfection were starved and then treated with nothing (control), LPLI (0.8 J/cm^2), or EGF (50 ng/ml), respectively. About 40 min after LPLI or EGF treatment, the cells were fixed, permeabilized, and stained for F-actin. Then, the percentage of cells generating at least one circular ruffle was determined. For each condition in (E) and (F), >100 cells were counted, and each represented the average value from three independent experiments (mean ± SD). Bars: 10 μm. [Color figure can be viewed in the online issue, which is available at www.interscience.wiley.com.]

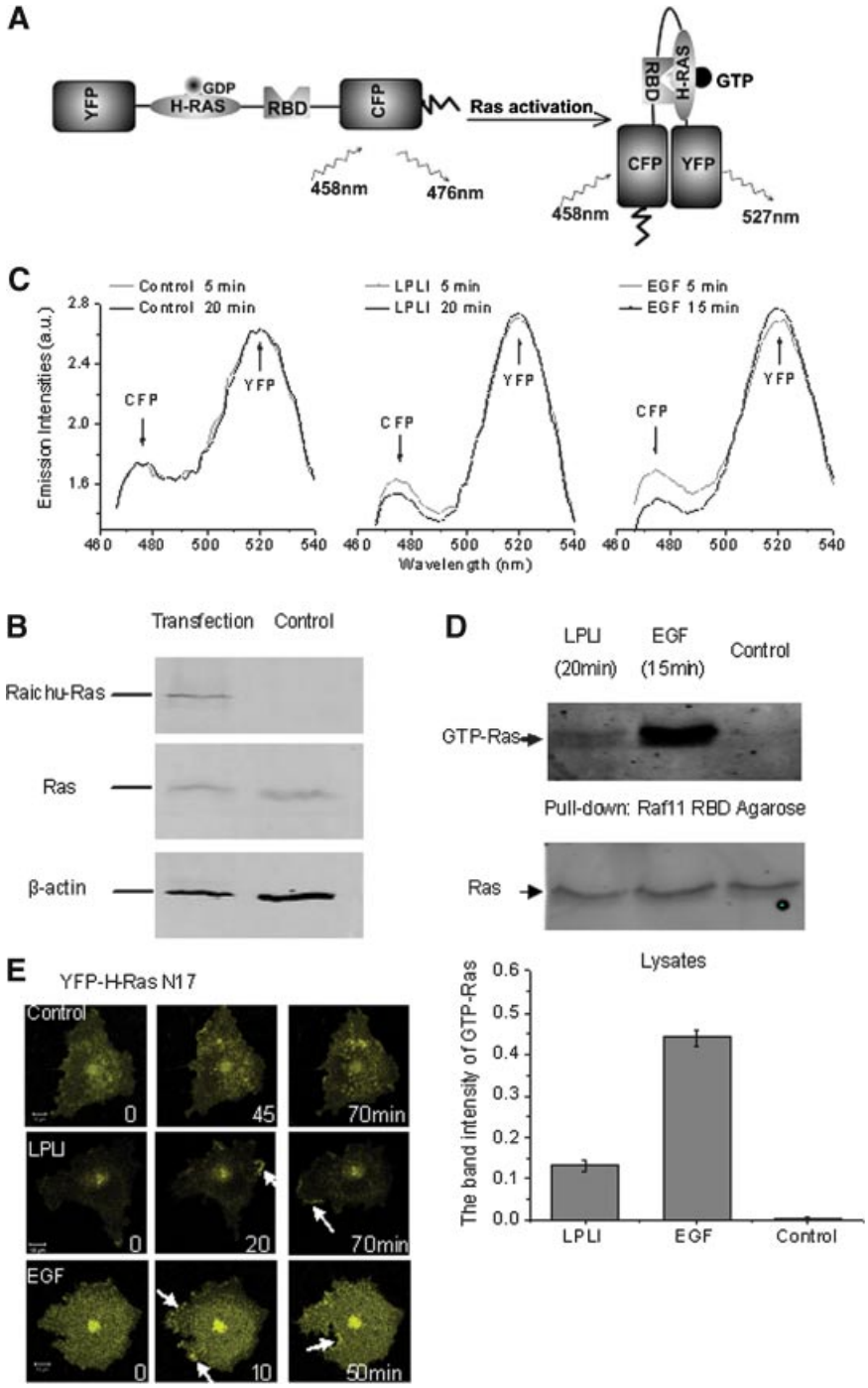

Fig. 3. The activation of Ras induced by LPLI. A: Schematic diagram of Raichu-Ras probe. Raichu-Ras was consisted of H-Ras, the Ras-binding domain of Raf (Raf RBD), C-terminal of K-Ras4B, and a pair of cyan and yellow fluorescent proteins (CFP and YFP). Intramolecular binding of GTP-Ras to Raf RBD upon EGF stimulation brings CFP close to YFP and increases FRET between CFP and YFP, which corresponding to a decrease in CFP emission peak and an increase in YFP emission peak. B: The expression of Raichu-Ras in COS-7 cells. COS-7 cells transfected with Raichu-Ras plasmid and control untransfected cells were lysed, and Raichu-Ras, Ras and actin proteins present in lysates were detected by Western blotting with anti-Ras and anti-β-actin antibodies. C: Spectrofluorometric analysis of Ras activation induced by LPLI and EGF in living cells. For detail methods see Materials and Methods Section. Control 5 min and Control 20 min mean 5 and 20 min after the control cells were transferred to microplate, respectively. LPLI 5 min and LPLI 20 min mean 5 and 20 min after LPLI, respectively. EGF 5 min and EGF 15 min mean 5 and 15 min after EGF, respectively. Results are representative of three independent replicates. D: COS-7 cells starved for 24 h were treated with nothing (control), LPLI for 20 min or EGF for 15 min, and then lysed. The GTP-bound Ras proteins (GTP-Ras) were affinity precipitated (pulled down) from the lysates by using Raf1 RBD Agarose beads. Supernatant after pull-down and aliquots of lysates were subjected to SDS–PAGE, transferred to nitrocellulose membranes, probed by Western blotting with monoclonal anti-Ras antibody. Quantification of GTP-Ras pulled-down by Agarose beads was shown in bottom. Values in the graph were mean band intensity (optical density) of GTP-Ras ± SD in three independent experiments. E: H-Ras (N17) inhibited the formation of LPLI-induced circular ruffles. COS-7 cells were transfected with YFP-H-Ras (N17) and starved for 24 h. Then the cells were treated with nothing (control), LPLI (0.8 J/cm^2), or EGF (50 ng/ml), respectively. The time-series images of control cell, LPLI- and EGF-treated cells were shown. Bars: 10 μm. [Color figure can be viewed in the online issue, which is available at www.interscience.wiley.com.]

effect of PI3K on the formation of LPLI-induced circular ruffles. After pretreatment with wortmannin (1 μM), PI3K inhibitor, and then irradiation with laser, the serum-starved cells transfected with GFP-H-Ras did not generate circular ruffles (Fig. 4A). The percentage of cells with circular ruffles after pretreatment with wortmannin was about 25%, consistent with the control group data (Fig. 4B). To further investigate the effects of wortmannin, decreasing concentration was used to determine how potently it inhibited circular ruffle formation. As the concentration reached 100 nM, circular ruffle production returned to 48% levels, revealing that wortmannin potently suppressed the formation of LPLI-induced circular ruffles in a dose-dependent manner.

In our previous study, the increased activation of PKC was confirmed during LPLI-induced cell proliferation (Gao et al., 2006). Subsequently, we investigated the effects of PKC activity on the formation of LPLI-induced circular ruffles. Gö 6983, PKC inhibitor, at 1 μM could completely inhibit the activation of PKC (Gao et al., 2006). COS-7 cells transfected with GFP-H-Ras were pre-incubated with 1 μM Gö 6983 for 30 min and then treated with LPLI. As shown in Figure 4C, Gö 6983 did not block circular ruffle formation. The percentage of cells with circular ruffles after pretreatment with Gö 6983 was nearly 74%, similar with the percentage of cells without Gö 6983 pretreatment (Fig. 4B). Thus, PKC activity did not affect the formation of circular ruffles.

Discussion

In this study, using confocal fluorescence microscope, we for the first time demonstrated the generation of circular ruffles when stimulated by LPLI in COS-7 cells (Fig. 2). The percentages of cells with circular ruffles were about 26% and 75% after irradiation in untransfected and H-Ras transfected COS-7 cells, respectively, which were largely enhanced compared with the control untreated cells (Fig. 2E,F). These results indicated that exogenous expression of wild-type GFP-H-Ras caused the generation of a small number of circular ruffles and that H-Ras protein was involved in the formation of these structures. These structures were characterized by the following: (1) expanding outside and changing into half ring-shaped or arc-shaped structures; (2) actin-based; (3) originating from membrane microdomains enriched in cholesterol. It is easy to

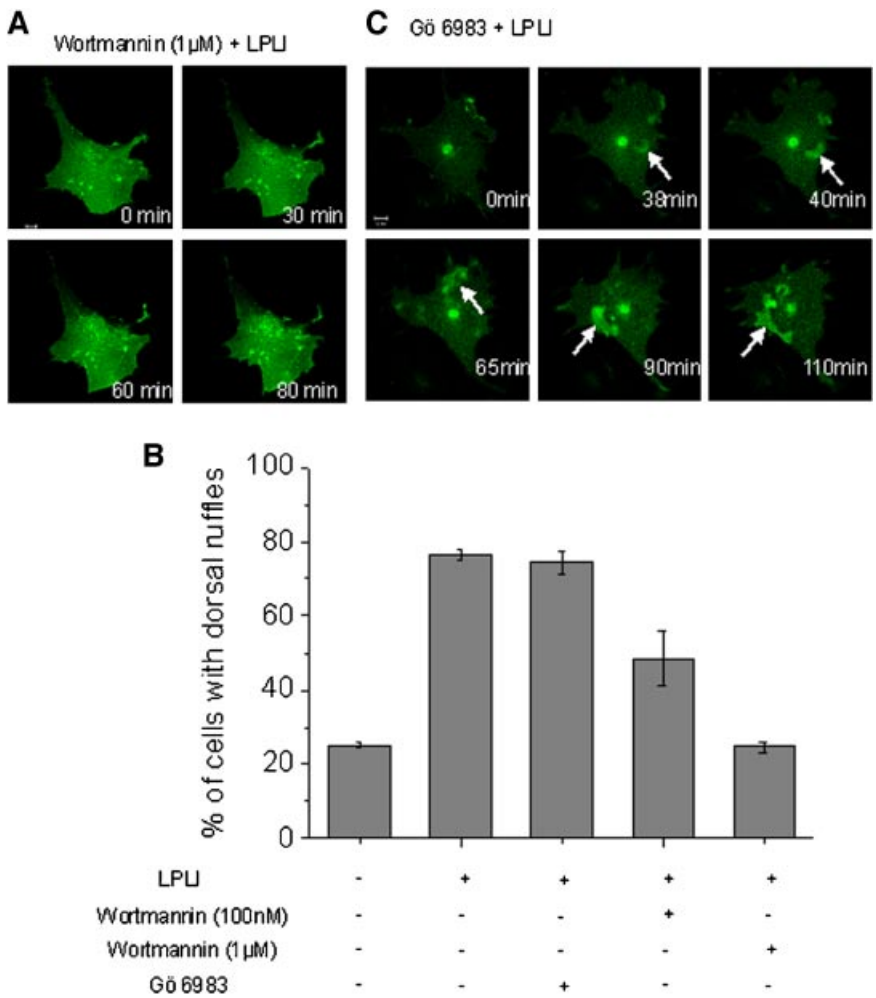

Fig. 4. The effects of PI3K and PKC on the generation of circular ruffles induced by LPLI. A: COS-7 cells expressing GFP-H-Ras were pretreated with wortmannin (1 μM) for 30 min and then treated with LPLI (0.8 J/cm^2). The time-series images after LPLI was shown. B: About 40 min after LPLI (0.8 J/cm^2) with or without wortmannin or Gö 6983 pretreatment, the cells were fixed and the percentage of cells generating at least one circular ruffle was determined. For each condition, >100 cells were counted, and each represented the average value from three independent experiments (mean ± SD). C: COS-7 cells expressing GFP-H-Ras were pretreated with Gö 6983 (1 μM) for 30 min and then treated with LPLI (0.8 J/cm^2). The time-series images after LPLI was shown. Bars: 10 μm. [Color figure can be viewed in the online issue, which is available at www.interscience.wiley.com.]

find that there are common characters between LPLI- and EGF-induced circular ruffles, which suggest the possibilities that LPLI induces the release of growth factor or that LPLI acts partly through activating the growth factor receptor. It has been reported that LPLI increases the expression of growth factors, like keratinocyte growth factor (KGF) (Gavish et al., 2004) and vascular endothelial growth factors (VEGF) (Kipshidze et al., 2001), and induces the phosphorylation of HGFR (Shefer et al., 2001). The formation of circular ruffles would facilitate the activation of static cells by changing cell shape, consistent with the opinion that circular ruffles helped reorganize the actin cytoskeleton and prepare static cells for motility (Krueger et al., 2003; Buccione et al., 2004).

What is the physiological relevance of LPLI-induced circular membrane ruffling? The formation of LPLI-induced circular ruffles may promote wound healing. LPLI has been shown to accelerate wound healing by promoting cell migration, proliferation and neovascularization, the important and necessary part of wound healing (Woodruff et al., 2004; Rezende et al., 2007). Proper wound healing requires orderly migration of multiple cell types, for example, epidermal cells, fibroblasts, and endothelial cells (Bandyopadhyay et al., 2006). The circular ruffles have been suggested to be important for epithelial cell migration and invasion, thus contributing to wound repair (Xiao et al., 2009). On the other hand, the formation of LPLI-induced circular ruffles may be beneficial for neural regeneration after injury. The researchers affirm the positive effect of LPLI on neural regeneration after trauma or in post-operative wounds (Mohammed et al., 2007). Neural stem cells (NSCs) have a capacity to migrate in a precise directed manner across great distances to injury sites in the central nervous system. Migration toward pathology is the first critical step in NSC engagement during regeneration (Imitola et al., 2004). The formation of circular ruffles upon LPLI would facilitate the static cells for subsequent motility. There are no experimental results at present that LPLI could induce circular ruffling in NSCs, but it is one possible mechanism for neural regeneration stimulated by LPLI. Thirdly, the circular ruffles could internalize large numbers of activated TPKRs from their surface for degradation (Orth et al., 2006). It is notable that the formation of these structures is less frequent in tumor cells than in some normal cells. The reported pancreatic and prostate tumor cell lines (BxPC3, PC3, HPAF, and PANC-1) form fewer waves ($<$5–10%) compared with mouse fibroblasts and primary human fibroblasts ($>$60%). Thus, tumor cells could not rapidly clear activated TPKRs from their surface for degradation, which may lead to unchecked growth (Orth et al., 2006; Orth and McNiven, 2006). In this study, we found that LPLI could induce the formation of circular ruffles, but in our previous studies, LPLI has been shown to increase the proliferation of tumor cells (human lung adenocarcinoma cells (Gao et al., 2006) and HeLa cells (Zhang et al., 2008)). Thus, LPLI is not the proper choice to inhibit cancer progression and the exact physiological relevance of LPLI-induced circular ruffling needs further investigation.

Our results for the first time showed that Ras could be activated by LPLI and the activation of Ras was required for the formation of LPLI-induced circular ruffles (Fig. 3). Using spectrofluorometric analysis and pull-down assay, the increased activation of Ras upon LPLI stimulation was detected. The weak activation of Ras after LPLI compared with EGF could increase cell viability step by step, which was more suitable for the damaged cells under abnormal condition. Expression of the negative H-Ras, YFP-H-Ras (N17), blocked the generation of circular ruffles induced by LPLI (Fig. 3E). Our result also showed that PI3K was required for the formation of circular ruffles induced by LPLI by using the well-established PI3K inhibitor wortmannin (Fig. 4). It has been reported that upon growth factors stimulation, TPKRs are activated and then the early effector kinases like PI3K and Src are activated. These lead to the activation of additional signaling proteins, such as the small GTPases Ras, Rac, and Rab5 (Buccione et al., 2004). There is other report that the small GTPases Ras, Rac, and Rab5 contribute to activation or recruitment of the components involved in circular ruffle formation, including PI3K, gelsolin, and WAVE1 (Lanzetti et al., 2004). Thus, which one of Ras or PI3K is the early effector during the formation of circular ruffles needs further investigation. According to our results and the existing views, we propose that Ras and PI3K form a positive feedback circuit during this process.

Another kinase, PKC, was activated in our previous study during LPLI-induced cell proliferation (Gao et al., 2006). We also investigated whether PKC contributed to circular ruffle formation. Our results demonstrated that the activity of PKC had no effect on the formation of circular ruffles (Fig. 3). Thus, LPLI activated the static cell through at least two different ways, one was the activation of signal pathways, like PKC, and the other was through inducing the formation of circular ruffles reported here which facilitated cell motility.

In conclusion, we for the first time demonstrated that LPLI could promote static cell activation through inducing the formation of circular ruffles. Ras was shown to be activated by LPLI and involved in the formation of LPLI-induced circular ruffles. These structures were regulated by H-Ras and PI3K. Much work must be done to seek the roles and regulation mechanisms of these structures. More importantly, the new sights into the cell motility induced by LPLI provide much new information for the mechanisms of biological effects of LPLI.

Acknowledgments

The authors thank Prof. Piero Crespo of Unidad de Biomedicina de la Universidad de Cantabria-CSIC in Spain for providing GFP-H-Ras plasmid, Prof. Thomas Schmidt of Leiden University in The Netherlands for providing YFP-H-Ras (N17) plasmid, and Prof. Michiyuki Matsuda of Osaka University in Japan for providing pRaichu-Ras plasmid. This work has been supported from grant National Natural Science Foundation of China, 30627003, 30870676, and from Natural Science Foundation of Guangdong Province, 7117865.

Literature Cited

Araki N, Hatae T, Hirohashi S. 2000. Actinin-4 is preferentially involved in circular ruffling and macropinocytosis in mouse macrophages: Analysis by fluorescence ratio imaging. J Cell Sci 113:3329–3340.

Bandyopadhyay B, Fan J, Guan S, Li Y, Chen M, Woodley DT, Li W. 2006. A "traffic control" role for TGFβ3: Orchestrating dermal and epidermal cell motility during wound healing. J Cell Biol 172:1093–1105.

Bivona TG, Philips MR. 2003. Ras pathway signaling on endomembranes. Curr Opin Cell Biol 15:136–142.

Buccione R, Orth JD, McNiven MA. 2004. Foot and mouth: Podosomes, invadopodia, and circular dorsal ruffles. Mol Cell Biol 5:647–657.

Chen C-H, Hung H-S, Hsu S-H. 2008. Low-energy laser irradiation increases endothelial cell proliferation, migration, and eNOS gene expression possibly via PI3K signal pathway. Lasers Surg Med 40:46–54.

Crespi D, Massa S, Basso V, Colombetti S, Mueller DL, Mondino A. 2002. Constitutive active p21ras enhances primary T cell responsiveness to Ca^{2+} signals without interfering with the induction of clonal anergy. Eur J Immunol 32:2500–2509.

Dowrick P, Kenworthy P, McCann B, Warn R. 1993. Circular ruffle formation and closure lead to macropinocytosis in hepatocyte growth factor/scatter factor-treated cells. Eur J Cell Biol 61:44–53.

Gao X, Chen T, Xing D, Wang F, Pei Y, Wei X. 2006. Single cell analysis of PKC activation during proliferation and apoptosis induced by laser irradiation. J Cell Physiol 206:441–448.

Gavish L, Asher Y, Becker Y, Kleinman Y. 2004. Low-level laser irradiation stimulates mitochondrial membrane potential and disperses subnuclear promyelocytic leukemia protein. Lasers Surg Med 35:369–376.

Imitola J, Raddassi K, Park KI, Mueller FJ, Nieto M, Teng YD, Frenkel D, Li J, Sidman RL, Walsh CA, Snyder EY, Khoury SJ. 2004. Directed migration of neural stem cells to sites of CNS injury by the stromal cell-derived factor 1alpha/CXC chemokine receptor 4 pathway. Proc Natl Acad Sci USA 101:18117–18122.

Janes PW, Ley SC, Magee AI. 1999. Aggregation of lipid rafts accompanies signaling via the T cell antigen receptor. J Cell Biol 147:447–461.

Jiang X, Sorkin A. 2002. Coordinated traffic of Grb2 and Ras during epidermal growth factor receptor endocytosis visualized in living cells. Mol Biol Cell 13:1522–1535.

Karu T. 1999. Primary and secondary mechanisms of action of visible to near-IR radiation on cells. J Photochem Photobiol B 49:1–17.

Kipshidze N, Nikolaychik V, Keelan MH, Shankar LR, Khanna A, Kornowski R, Leon M, Moses J. 2001. Low-power helium: Neon laser irradiation enhances production of vascular endothelial growth factor and promotes growth of endothelial cells in vitro. Lasers Surg Med 28:355–364.

Krueger EW, Orth JD, Cao H, McNiven MA. 2003. A dynamin-cortactin-Arp2/3 complex mediates actin reorganization in growth factor-stimulated cells. Mol Biol Cell 14:1085–1096.

Kupzig S, Walker SA, Cullen PJ. 2005. The frequencies of calcium oscillations are optimized for efficient calcium-mediated activation of Ras and the ERK/MAPK cascade. Proc Natl Acad Sci USA 102:7577–7582.

Lanzetti L, Palamidessi A, Areces L, Scita G, Di Fiore PP. 2004. Rab5 is a signalling GTPase involved in actin remodeling by receptor tyrosine kinases. Nature 429:309–314.

Mellstrom K, Heldin CH, Westermark B. 1988. Induction of circular membrane ruffling on human fibroblasts by platelet-derived growth factor. Exp Cell Res 177:347–359.

Mochizuki N, Yamashita S, Kurokawa K, Ohba Y, Nagai T, Miyawaki A, Matsuda M. 2001. Spatio-temporal images of growth-factor-induced activation of Ras and Rap1. Nature 411:1065–1068.

Mohammed IF, Al-Mustawfi N, Kaka LN. 2007. Promotion of regenerative processes in injured peripheral nerve induced by low-level laser therapy. Photomed Laser Surg 25:107–111.

Orth JD, McNiven MA. 2006. Get Off My Back! Rapid receptor internalization through circular dorsal ruffles. Cancer Res 66:11094–11096.

Orth JD, Krueger EW, McNiven MA. s2003.A dynamin-cortactin-N-WASp complex mediates the sequestration and macropinocytic internalization of the EGF-receptor via dorsal ruffles/waves. Mol Biol Cell 14:A465.

Orth JD, Krueger EW, Weller SG, McNiven MA. 2006. A novel endocytic mechanism of epidermal growth factor receptor sequestration and internalization. Cancer Res 66:3603–3610.

Rezende SB, Ribeiro MS, Nunez SC, Garcia VG, Maldonado EP. 2007. Effects of a single near-infrared laser treatment on cutaneous wound healing: Biometrical and histological study in rats. J Photochem Photobiol B 87:145–153.

Safiejko-Mroczka B, Bell PBJ. 2001. Reorganization of the actin cytoskeleton in the protruding lamellae of human fibroblasts. Cell Motil Cytoskeleton 50:13–32.

Shefer G, Oron U, Irintchev A, Wernig A, Halevy O. 2001. Skeletal muscle cell activation by low-energy laser irradiation: A role for the MAPK/ERK pathway. J Cell Physiol 187:73–80.

Shefer G, Partridge TA, Heslop L, Gross JG, Oron U, Halevy O. 2002. Low-energy laser irradiation promotes the survival and cell cycle entry of skeletal muscle satellite cells. J Cell Sci 115:1461–1469.

Shefer G, Barash I, Oron U, Halevy O. 2003. Low-energy laser irradiation enhances de novo protein synthesis via its effects on translation-regulatory proteins in skeletal muscle myoblasts. Biochim Biophys Acta 1593:131–139.

Shinohara M, Terada Y, Iwamatsu A, Shinohara A, Mochizuki N, Higuchi M, Gotoh Y, Ihara S, Nagata S, Itoh H, Fukui Y, Jessberger R. 2002. SWAP-70 is a guanine-nucleotide-exchange factor that mediates signalling of membrane ruffling. Nature 416:759–763.

Tuby H, Maltz L, Oron U. 2007. Low-Level laser irradiation (LLLI) promotes proliferation of mesenchymal and cardiac stem cells in culture. Lasers Surg Med 39:373–378.

Woodruff LD, Bounkeo JM, Brannon WM, Dawes KS, Barham CD, Waddell DL, Enwemeka CS. 2004. The efficacy of laser therapy in wound repair: A meta-analysis of the literature. Photomed Laser Surg 22:241–247.

Xiao H, Eves R, Yeh C, Kan W, Xu F, Mak AS, Liu M. 2009. Phorbol ester-induced podosomes in normal human bronchial epithelial cells. J Cell Physiol 218:366–375.

Zhang J, Xing D, Gao X. 2008. Low-power laser irradiation activates Src tyrosine kinase through reactive oxygen species-mediated signaling pathway. J Cell Physiol 217:518–528.